Proceedings of the 26th International Conference on Offshore Mechanics and Artic Engineering
OMAE2007
June 10-15, 2007, San Diego, California, USA

OMAE2007-29618

THE EFFECT OF STRUCTURAL COMPLIANCE ON FATIGUE CRACK GROWTH IN JACKET STRUCTURES

Ronald Schneider
MMI Engineering Ltd.
Warrington, UK

David J Sanderson
MMI Engineering Ltd.
Warrington, UK

Simon D Thurlbeck
MMI Engineering Ltd.
Warrington, UK

ABSTRACT

Quantifying the fatigue crack growth and remaining life in joints making up jacket structures forms one of the basic requirements of a sub sea structural integrity assurance scheme. The accurate prediction of the likely failure time of welds allows a realistic estimate of the risk of structural collapse at any stage in a structure's life. It is current practice to consider the welds making up the member as individual components rather than looking at the whole compliant system of welds, joints, members, and structural framing arrangement. In this approach, the nominal loads in any one member are determined from an analysis of the undamaged structure and are then applied to a crack growth solution using handbook stress intensity factor solutions to determine the fatigue life of that component. This method assumes that the applied load is purely load-controlled whereas in reality it is a combination of both load and displacement controlled.

A study was performed to investigate the influence of the surrounding structure on crack growth in tubular members located in jacket structures. The aim of the study was to verify whether the traditional approach, which uses stresses from undamaged structures to evaluate crack growth in individual components, is appropriate.

The findings of the study showed that structural compliance has only a beneficial effect on fatigue growth in the latter stage of the crack growth process with crack lengths greater than 40% circumference. It was shown that the beneficial effect of structural compliance on fatigue crack growth in the later stage of the growth process does not significantly increase the overall fatigue life. It was concluded, that the current approach, which uses stresses from undamaged structures to evaluate crack growth in individual components, is valid and safe to use.

1 INTRODUCTION

Quantifying the fatigue crack growth and remaining life in joints making up jacket structures forms one of the basic requirements of a sub sea structural integrity assurance scheme. The accurate prediction of the likely time to failure allows realistic estimates to be made of the risk of structural collapse as a result of weld failure at any stage in a structure's life.

When making such predictions for the likelihood of a member failure it is usual to consider the welds making up the member as individual "stand-alone" components rather than looking at the whole compliant system of welds, joints, members, and structural framing arrangement. In this approach the nominal loads in any one member are determined from an analysis of the undamaged structure and they are applied to a crack growth solution using handbook stress intensity factor solutions (SIF) and a suitable fatigue crack growth law to determine the remaining fatigue life of a cracked component.

This method does not capture the effects on local compliance of introducing a defect which is to say that the loading is treated as purely load controlled when in fact it is a combination of both load and displacement controlled.

Previous work [1] carried out involved the stress analysis of five jackets, nominally designed for the same Southern North Sea location, but with different bracing configurations, namely X-braced, K and inverted K-braced, diamond braced and diagonally braced. The analyses involved the examination of the stress distributions before and after damage had occurred to each of the members in the jackets. The effects of the stress redistribution were input into reliability assessments to evaluate the significance of ignoring their effects in reliability analyses.

It is apparent that some significant redistribution of loads occurs in a structure if a member has been fully severed. The effect of partial member failure on redistributed stresses in a structure only becomes significant in the latter stages of member damage. In fact, until the crack has propagated through 70% of the member's cross sectional area, the effects of stress redistribution on the overall structure are considered negligible [1].

The effects of this global redistribution on the local loading within a cracked, but not fully severed, member are unclear. Furthermore, the influence of the constraint of the surrounding structure on conditions at the location of the crack is also

unknown. This level of constraint could vary between structures of differing structural redundancy.

It is uncertain whether including the influence of the surrounding structure on the loads within a cracked member or joint will have a significant effect on the calculation of remaining life estimates compared with ignoring the effect and using current remaining life calculation techniques.

The work described in this paper sought to investigate the influence of the surrounding structure on crack growth in tubular members located in jacket structures and was intended to verify whether the current approach, which uses stresses from undamaged structures to evaluate crack growth in individual components, is appropriate.

The work focused on whether the assumptions made by such an approach provide a safe assessment method and indicate the levels of conservatism that may be present.

2 METHODOLOGY

A study was undertaken on two jacket models which were based on the same baseline structure but with different bracing configurations, namely a high redundancy X-braced configuration and the low redundancy single diagonal braced configuration. Two members were selected from each jacket at differing vertical bays in the structure. Per selected member a number of semi-elliptical external circumferential surface cracks and circumferential through-wall cracks of different geometry were introduced. To aid modelling, the cracks were assumed to develop in circumferential closure welds rather than tubular joint welds.

A detailed finite element (FE) model was created for each of the different member sizes and crack geometries. Two different approaches were used to evaluate the stress intensity factors (SIFs) for the different cracked members:

1. For each of the cracked components, SIFs were determined for the pure unit tension and pure unit bending conditions. Based on these results it was possible to determine SIFs for any combination of axial force and bending moment utilising elastic superposition principles. This was valid since linear elastic fracture mechanics (LEFM) methods were used.

   A global structural analysis of both undamaged jacket structures subjected to a reference load set (RLS) was performed. Axial forces and resultant bending moments were extracted at the correct location of the cracked sections and than used to determine the corresponding SIFs for each cracked tube utilising the reference SIFs calculated for pure unit tension and pure unit bending. This approach is referred to as the ***component case*** and conforms to the guidelines outlined in BS 7910 [2].

2. Each cracked tube model was incorporated into the corresponding jacket model at the correct locations. The cracked tubes were oriented to maximise crack opening as dictated by the vector defining the resultant bending moment in the undamaged structure. The "damaged" jacket models were subsequently loaded with the RLS and the SIFs were directly calculated from the analysis. This approach is referred to as the ***structural system case***.

Based on the results of the above described analyses it was possible to quantify relative differences or shifts in the SIF estimates calculated with both approaches.

Note that the first of the described approaches could have been undertaken using readily available handbook solutions such as BS 7910 [2]. However, by using the same cracked component models for the calculation of the SIFs in both approaches, inconsistencies in the derivation of SIF due to the FE mesh, SIF calculation method etc. were eliminated.

3 JACKET MODELS

3.1 Jacket Description

The current work built on, and utilised, structural models developed for a previous study on stress redistribution [1]. The previous study considered a generic four-legged jacket structure designed for the same Southern North Sea location but with different bracing configuration, namely X-braced, K-braced, inverted K-braced, diamond braced and single diagonal braced, as shown in Figure 1. The jacket structure is made up of circular hollow sections (CHS) and it stands in approximately 45m of water. For the current study it was decided to use the high redundancy X-braced jacket and the low redundancy diagonally braced jacket.

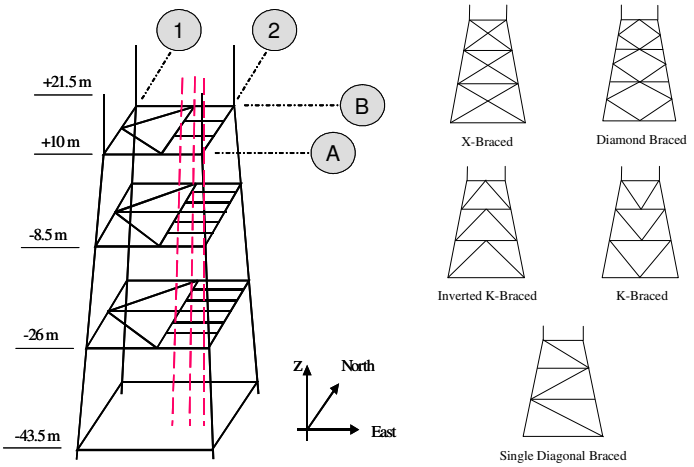

Figure 1: Generic Jacket Structure and Different Bracing Schemes

The jacket structure had the following characteristics:

- topside mass = 1200 t
- 18 well conductors
- 8 Piles (2 per leg)
- Batter 6.2° North and 1.6° East
- 3 conductor frames

3.2 Element Formulation and Material Model

The jacket structures were modelled using ABAQUS FE software [3]. The models comprised 2-node linear beam elements (B31 elements). The applied mesh refinement was relatively high with a typical element length of 1m.

The material model used in the current study was based upon typical structural steel. Linear elastic material behaviour was adopted since LEFM methods were applied throughout the study. The values adopted for Young's modulus and Poisson's Ratio are as follows:

- Young's modulus $E = 2.1 \cdot 10^5\ N/mm^2$
- Poisson's ratio $v = 0.3$

3.3 Loading

The topside was represented in the generic structure as a point mass located at the centre of gravity of the topside. The point mass element was tied into the structure at the stab-in points using beam type multi-point constraints.

The environmental load applied to the structure was based on the 100-year storm wave, current and wind. The wind loading was idealised as a concentrated load applied at the geometric centre of the four stab-in points. The wind load corresponded to the force that would be introduced into the structure as a result of the wind resistance of the topside. The current-induced load and the wave-induced loads as well as the buoyancy load were determined using ABAQUS/Aqua [4]. The RLS was derived from the 100-year storm load that resulted in the greatest base shear in the jacket.

This approach ensured that the structure remained in the elastic regime since the jacket structures were designed to exhibit an elastic response when exposed to a 100-year storm. For the current project it was decided to consider a storm from platform East (see Figure 1).

3.4 Selection of Members for Current Study

The members investigated in the current study were selected based on the findings of a previous study [5] undertaken to assess the applicability of online monitoring to different classes of North Sea jackets. This study also utilised the jacket models developed for the stress redistribution study [1]. The online monitoring technique identifies damage in jacket structures by measuring changes in the frequency response of platforms subjected to cyclic wave motion since a severed member causes a reduction in overall stiffness which in turn reduces the corresponding response frequency.

For the current project members from Frame A (see Figure 1) were selected that produced the largest changes in the fundamental frequency in direction parallel to the face in which the members were severed (i.e. South/East direction). These members contribute largely to the stiffness of the structure and it was therefore expected that by partially severing these members a considerable redistribution of stresses would occur in the structure. Additionally, the selected members had to be in tension for the given RLS. The selected members are shown in Figure 2.

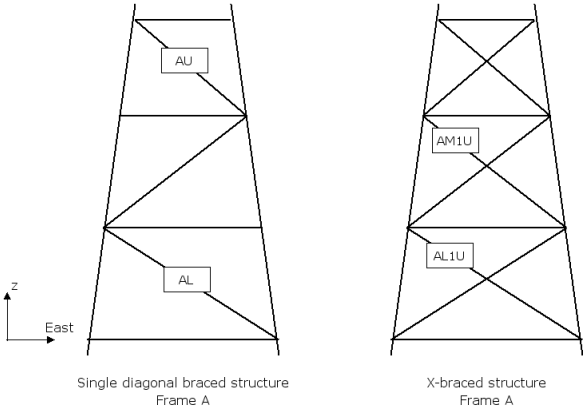

Figure 2: Member Location and Identifiers

The section sizes of the selected members are shown in Table 1.

Table 1: Section Properties of Selected Members

Member ID	Diameter D (m)	Wall Thickness t (m)
AL	1.35	0.045
AU	1.10	0.07
AL1U	0.85	0.04
AM1U	0.75	0.055

4 CRACKED COMPONENT MODELS

4.1 Dimensions

A total of 5 cracked component models with semi-elliptical external circumferential surface cracks of different geometry and 4 cracked component models with circumferential through-wall cracks of different length were generated for each selected member using ABAQUS [3].

In each case, the semi-elliptical external circumferential surface cracks had a fixed aspect ratio $a/c = 0.2$ where c is half the crack length and a is the crack depth (see Figure 3). Based on the a/c ratio, 5 different models with a/t ratios of 0.1, 0.3, 0.5, 0.7 and 0.9 were implemented per selected member where t is the wall thickness of the member. The circumferential through-wall crack length $2a$ (see Figure 4) varied for each member from 20%, 40%, 60% to 80% circumference.

The length of the component models was selected such that the influence of boundary effects when coupled on both ends with

beam elements was kept to a minimum. It was shown [6] that for component models with semi-elliptical surface cracks a length-to-outer diameter ratio $l/D \geq 1.0$ and for component models with through-wall cracks a length-to-outer diameter ratio $l/D \geq 3.0$ was sufficient.

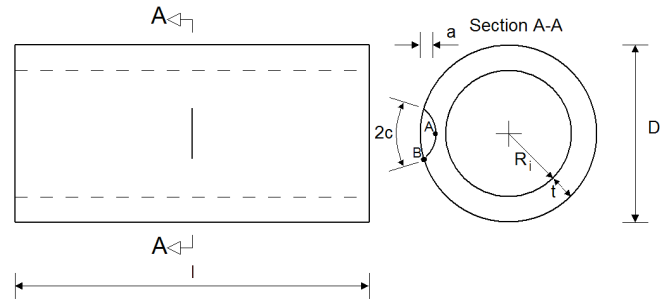

Figure 3: Tubular Member with Circumferential External Semi-Elliptical Surface Crack

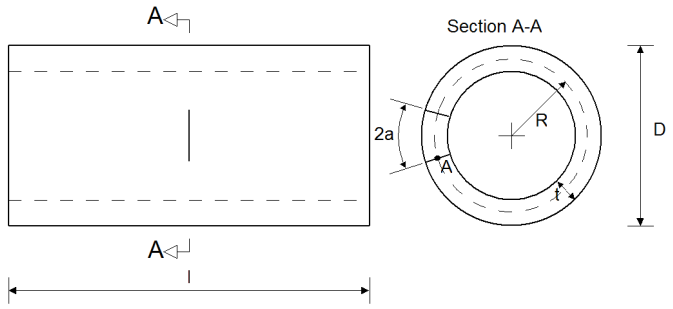

Figure 4: Tubular Member with Circumferential Through-Wall Crack

4.2 Element Formulation and Material Model

All cracked components were modelled with 20-node quadratic brick element with reduced integration (C3D20R) provided by ABAQUS [3]. To ensure consistency, the material model implemented for the cracked components corresponds to the model used for the beam elements making up the jacket model (see Section 3.2).

4.3 Crack Tip Singularity Modelling

In this calculation a $1/\sqrt{r}$ strain singularity suitable for LEFM application [7] was adopted where r is the distance from the crack tip. This was achieved by using quadratic elements (see Section 4.2) with collapsed element sides and single nodes on the side which is connected to the crack tip [7]. Additionally, the mid-side nodes on the sides connected to the crack tip were moved to the 1/4 points nearest to the crack tip [7].

4.4 Calculation of SIFs from *J*-Integral Estimates

ABAQUS [3] implements the virtual crack extension method which is a procedure to provide estimates of the *J*-integral. In each FE analysis the *J*-integral for a defined number of contours was calculated at each node along the crack line. In the current project 5 different contours at each node along the crack line gave sufficient path-independence [6].

The *J*-Integral *J* could subsequently be related to the SIF, K_I, through the following equation [8]:

$$K_I = \sqrt{JE'} \tag{1}$$

where $E' = E$ for plane stress and $E' = E / (1-\nu^2)$ for plane strain [8]. In the current study SIFs were determined using Equation (1) and the average value of the corresponding *J*-integrals.

The quality of the cracked component models, i.e. quality of *J*-integral estimates, was evaluated in a number of verification studies [6] comparing SIFs derived from *J*-integral estimates against handbook solutions (see [2],[9]) for simple load cases. The studies concluded that for semi-elliptical surface cracks the best *J*-integral estimates were achieved when plane strain conditions were assumed for the deepest point along the crack line and plane stress conditions were assumed for the end point of the crack line. For through-wall cracks it was shown that assumed plane stress conditions gave the best results for the point at mid-height of the crack tip line. The FE results agreed within 5% with the handbook solutions (see [2],[9]) when assuming these stress/strain conditions. This was considered to validate the FE mesh.

5 INTEGRATION OF CRACKED COMPONENT MODELS INTO JACKET MODELS

5.1 Location of Closure Welds

In the current study the cracks were assumed to develop in circumferential closure welds rather than in joint welds. This was decided to simplify the modelling process. It was assumed that each joint in the jacket structure was made up of prefabricated nodes as shown in Figure 5.

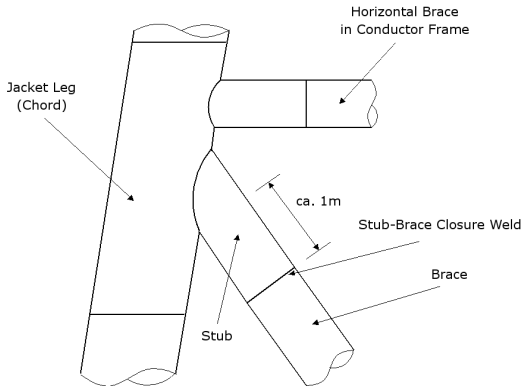

Figure 5: Prefabricated Node

In each case, the length of the stub for the leg-brace connection which determines the location of the closure weld being studied was taken to be approximately 1m (see Figure 5). The location of the closure welds in turn determined the position of the cracked component model in the overall jacket model. The

cracked tubes were oriented to maximise crack opening as dictated by the vector defining the resultant bending moment in the undamaged structure. Figure 6 shows the x-braced jacket model with the integrated cracked component model at the assumed location of the closure weld for member AL1U.

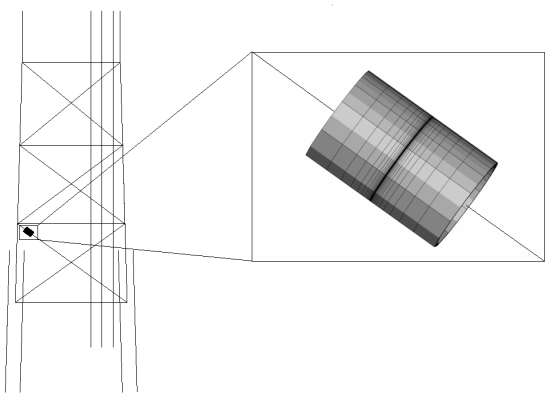

Figure 6: Cracked Component Model incorporated into Jacket Model (Member Al1U)

5.2 Coupling of Component Models with Beam Elements

The connection between the cracked component models and the reference nodes (end nodes of adjacent beam elements) was achieved by applying coupling constraints which are provided by ABAQUS [3]. Two different types of coupling constraints suitable for connecting solid elements and with the reference nodes are implemented in ABAQUS [3]:

1. Kinematic coupling
2. Distributing coupling

Both types of coupling constraint have the common purpose of coupling the motion of a collection of nodes on a surface to the motion of a reference node. A detailed description of the coupling constraints can be found in the ABAQUS user's manual [7].

In the present study, both types of coupling constraints have been used. It was found [6] that the use of kinematic couplings with radially unconstrained degrees of freedom gave the best SIF estimates for components with semi-elliptical surface cracks. In the case of components with though-wall cracks the most accurate results were obtained when distributing couplings were used.

6 ANALYSIS RESULTS

The results obtained in the present study are tabulated below. The tables summarise the SIFs calculated for each member with external semi-elliptical circumferential surface cracks and circumferential through-wall cracks of different size. Each table shows the SIFs for the component case, K_1, (current industry-standard method, ignoring structural compliance) and for the structural system case, K_2, (which investigates the effects of structural compliance). In each case, the component SIF, K_1, was calculated using the force resultants from the undamaged structure utilising elastic superposition. For the structural system case, the SIF, K_2, was calculated directly from the analysis. The tables also show the ratio K_2/K_1 indicating the relative difference between the component case and the structural system case.

6.1 SIF versus Increasing Crack Size for Surface Cracks

In the case of semi-elliptical surface cracks, the SIFs calculated for each selected member are summarised in Table 2 to Table 9 for the deepest point of the crack and the crack ends, respectively. The SIFs are shown with respect to increasing crack size. The crack size is given in terms of the non-dimensional ratio a/t where a is the crack depth and t is the wall thickness of the corresponding member (see Figure 3). It can be seen from Table 2 to Table 9 that for each member the ratio $K_2/K_1 \leq 1.01$. This difference is regarded to be negligible

Table 2: SIFs vs Crack Size at Deepest Point of Crack (Member AL)

a/t [/]	K_1 [MPa√m] (component case)	K_2 [MPa√m] (structural system case)	K_2/K_1
0.1	18.0	18.0	1.00
0.3	35.3	35.3	1.00
0.5	55.6	55.6	1.00
0.7	78.8	78.8	1.00
0.9	98.7	98.9	1.00

Table 3: SIFs vs Crack Size at Surface Point of Crack (Member AL)

a/t [/]	K_1 [MPa√m] (component case)	K_2 [MPa√m] (structural system case)	K_2/K_1
0.1	9.1	9.1	1.00
0.3	17.7	17.7	1.00
0.5	28.1	28.1	1.00
0.7	41.0	41.1	1.00
0.9	59.8	59.9	1.00

Table 4: SIFs vs Crack Size at Deepest Point of Crack (Member AU)

a/t [/]	K_1 [MPa√m] (component case)	K_2 [MPa√m] (structural system case)	K_2/K_1
0.1	8.4	8.4	1.00
0.3	16.4	16.4	1.00
0.5	25.6	25.7	1.00
0.7	36.4	36.5	1.00
0.9	48.2	48.6	1.01

Table 5: SIFs vs Crack Size at Surface Point of Crack (Member AU)

a/t [/]	K_1 [MPa√m] (component case)	K_2 [MPa√m] (structural system case)	K_2/K_1
0.1	4.2	4.2	1.00
0.3	7.3	7.3	1.00
0.5	12.7	12.7	1.00
0.7	16.5	16.6	1.00
0.9	22.2	22.3	1.01

Table 6: SIFs vs Crack Size at Deepest Point of Crack (Member AL1U)

a/t [/]	K_1 [MPa√m] (component case)	K_2 [MPa√m] (structural system case)	K_2/K_1
0.1	16.2	16.2	1.00
0.3	31.8	31.8	1.00
0.5	50.1	50.1	1.00
0.7	71.4	71.4	1.00
0.9	92.6	92.7	1.00

Table 7: SIFs vs Crack Size at Surface Point of Crack (Member AL1U)

a/t [/]	K_1 [MPa√m] (component case)	K_2 [MPa√m] (structural system case)	K_2/K_1
0.1	7.7	7.8	1.00
0.3	17.4	17.3	1.00
0.5	23.6	23.6	1.00
0.7	35.4	35.4	1.00
0.9	49.9	49.9	1.00

Table 8: SIFs vs Crack Size at DeepestPoint of Crack (Member AM1U)

a/t [/]	K_1 [MPa√m] (component case)	K_2 [MPa√m] (structural system case)	K_2/K_1
0.1	11.3	11.3	1.00
0.3	22.1	22.1	1.00
0.5	34.7	34.7	1.00
0.7	49.5	49.6	1.00
0.9	67.1	67.4	1.00

Table 9: SIFs vs Crack Size at Surface Point of Crack (Member AM1U)

a/t [/]	K_1 [MPa√m] (component case)	K_2 [MPa√m] (structural system case)	K_2/K_1
0.1	5.7	5.8	1.01
0.3	11.6	11.6	1.00
0.5	17.0	17.0	1.00
0.7	23.0	23.0	1.00
0.9	32.4	32.6	1.00

6.2 SIF versus Increasing Crack Size for Through-Wall Cracks

In the case of through-wall cracks, the SIFs calculated for each selected member are summarised in Table 10 to Table 13 for the point at mid-thickness of the tube wall. The SIFs are shown with respect to increasing crack size. The crack size is given in terms of the non-dimensional ratio $a/(\pi R)$ where a is half the crack length and R is the mean radius of the corresponding member, as shown in Figure 4.

The SIF estimates obtained from the structural system case differ from the component case with varying magnitude (see Table 10 to Table 13). It can also be seen from Table 10 to Table 13 that for each member in the case of ratio $a/(\pi R) = 0.2$, the absolute deviation of the SIF calculated for the structural system case compared to the component case is less than 1% which is regarded as negligible.

Table 10 to Table 13 show that up to a crack length $2a$ of 40% circumference the ratio K_2/K_1 range from 0.92 to 1.03. For cracks longer than 60% circumference the SIF estimates for the structural system case reduce significantly when compared to the the component case. In the case of $a/(\pi R) = 0.8$, the reduction is approximately 50%.

The deviation of the SIF estimates for cracks greater than 60% circumference can clearly be attributed to the structural compliance. A significant reduction in section reduces the axial and bending stiffness of the member which in turn leads to load shedding throughout the remainder of the structure. Therefore, the load attracted by the cracked member decreases and in turn the SIF decreases as well.

Table 10: SIFs vs Crack Size (Member AL)

a/(πR) [/]	K_1 [MPa√m] (component case)	K_2 [MPa√m] (structural system case)	K_2/K_1
0.2	285.3	288.0	1.01
0.4	520.4	517.3	0.99
0.6	754.8	565.1	0.75
0.8	1918.6	904.7	0.47

Table 11: SIFs vs Crack Size (Member AU)

a/(πR) [/]	K_1 [MPa√m] (component case)	K_2 [MPa√m] (structural system case)	K_2/K_1
0.2	79.1	80.0	1.01
0.4	156.2	161.5	1.03
0.6	255.3	237.6	0.93
0.8	518.9	269.5	0.52

Table 12: SIFs vs Crack Size (Member AL1U)

a/(πR) [/]	K_1 [MPa√m] (component case)	K_2 [MPa√m] (structural system case)	K_2/K_1
0.2	192.0	189.6	0.99
0.4	383.4	354.2	0.92
0.6	600.0	467.6	0.78
0.8	1029.0	528.7	0.51

Table 13: SIFs vs Crack Size (Member AM1U)

a/(πR) [/]	K_1 [MPa√m] (component case)	K_2 [MPa√m] (structural system case)	K_2/K_1
0.2	96.7	96.3	1.00
0.4	201.4	192.1	0.95
0.6	347.8	283.5	0.82
0.8	597.2	288.3	0.48

7 ASSESSMENT OF REMNANT FATIGUE LIFE

An assessment of the remnant fatigue life of a member with a circumferential through-wall crack with a length of 20% circumference was carried out in order to quantify the effect of structural compliance. The section properties of member AM1U (see Table 1) and the material parameters defined in Section 3.2 were used. The following assumption was made:

$$K_2 / K_1 = \Delta K_2 / \Delta K_1 \tag{2}$$

where K_1 is the SIF for the component case, K_2 is the SIF for the structural system case, ΔK_1 is the SIF range for the component case, ΔK_2 is the SIF range for the structural system case. The correlation between the SIF ratio K_2/K_1 and the crack size $a/(\pi R)$ used in the assessment is shown in Figure 7 and is based on the results summarised in Table 13.

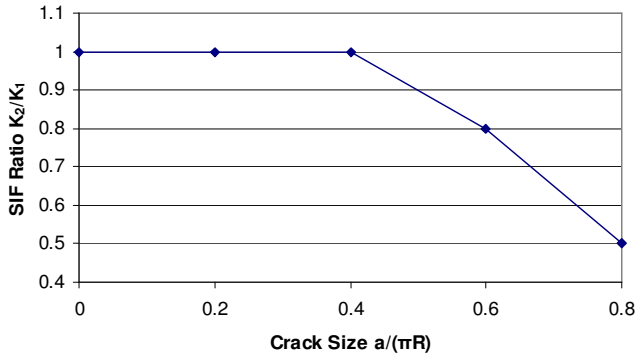

Figure 7: SIF Ratio vs Crack Size

It follows from Equation (2) and the correlation shown in Figure 7 that:

$$\begin{aligned} \Delta K_2 &= \Delta K_1 && \text{for } 0.2\pi R \le a \le 0.4\pi R \\ \Delta K_2 &= (1.4 - a/(\pi R))\Delta K_1 && \text{for } 0.4\pi R \le a \le 0.6\pi R \\ \Delta K_2 &= (1.7 - 1.5a/(\pi R))\Delta K_1 && \text{for } 0.6\pi R \le a \le 0.8\pi R \end{aligned} \tag{3}$$

The fatigue growth rate da/dN was evaluated using the Paris law [2].

$$da / dN = A(\Delta K)^m \tag{4}$$

where ΔK is the applied SIF range, A and m are constants which depend on the material and the applied conditions, including environment and cyclic frequency. A simplified fatigue crack growth law for steels operating in marine environments was used which recommends the following values for A and m [2]:

- $A = 2.3 \cdot 10^{-12}$ N/mm^2
- $m = 3$

Separating variables and integrating gives:

$$N = \frac{1}{A}\int_{a_i}^{a_f} \frac{1}{(\Delta K)^m} da \tag{5}$$

where N is the remnant fatigue in cycles, $2a_i$ is the initial crack size and $2a_f$ is the finial crack size. The initial crack size $2a_i$ was chosen to be 20% circumference and the finial crack size $2a_f$ was chosen to be 80% circumference.

The SIF range ΔK is a function of structural geometry, stress range and instantaneous crack size. The SIF solution for circumferential through-wall cracks provided in BS 7910 [2] was used in the current assessment. The effects of stress intensity magnification, stress concentration and stress magnification due to misalignment were ignored. Furthermore, it was assumed that the crack was subjected only to primary membrane stress with a stress range ΔP_m of 1 N/mm^2.

Table 14 summarises the remnant fatigue life in terms of cycles N for the component case, N_1, and the structural system case, N_2, derived using the SIF solution for circumferential through-wall cracks provided in BS 7910 [2] and Equations (3) and (5). Table 14 also shows the ratio N_2/N_1 indicating the relative change in remnant fatigue life when comparing the component case with the structural system case.

Table 14: Remnant Fatigue Life

Crack Size Range	N_1 [cycles] (component case)	N_2 [cycles] (structural system case)	N_2/N_1
$0.2\pi R \le a \le 0.4\pi R$	$3.31 \cdot 10^8$	$3.31 \cdot 10^8$	1.00
$0.4\pi R \le a \le 0.6\pi R$	$4.29 \cdot 10^7$	$5.46 \cdot 10^7$	1.27
$0.6\pi R \le a \le 0.8\pi R$	$8.14 \cdot 10^6$	$2.82 \cdot 10^7$	3.47
Total	$3.82 \cdot 10^8$	$4.13 \cdot 10^8$	1.08

It can be seen from Table 14 that the number of cycles necessary to grow the crack from 40% circumference to 60% circumference is approximately 30% larger when comparing the component case (including structural compliance) with the structural system case (ignoring structural compliance). The number of cycles necessary to grow the crack from 40% circumference to 60% circumference is approximately 250% larger when structural compliance is taken into account. The overall increase in remnant fatigue life, however, is only approximately 8%. This is due to the fact that for the number of cycles necessary to grow the crack from 40% circumference to 60% circumference or from 60% circumference to 80% circumference is of an order of magnitude smaller when compared with the number of cycles necessary to grow the crack from 20% circumference to 40% circumference (see Table 14). Therefore, a change in the number of cycles in the later stage of crack growth process does not significantly affect the overall number of cycles. This is shown schematically in Figure 8.

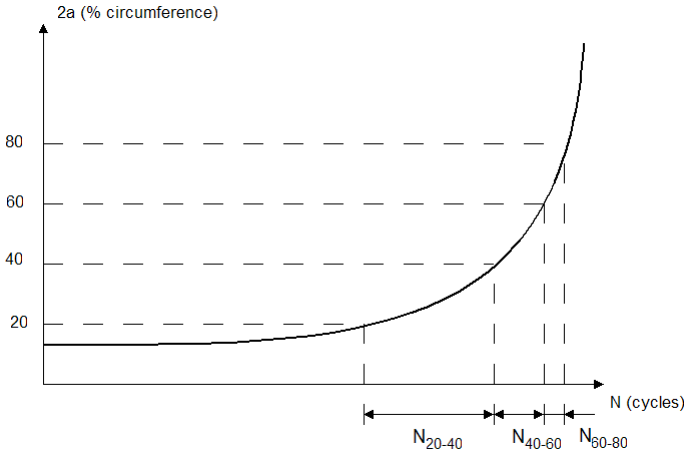

Figure 8: Crack Size vs Remnant Fatigue Life

8 CONCLUSIONS

It was found that in the case of surface cracks the SIFs calculated for the structural system case and for the component case diverge only marginally (less than 1%). The surface cracks do not change the axial and bending stiffness of the members sufficiently to produce any load redistribution in the structure and unloading of the cracked member. The effect of structural compliance is in this case negligible

In the case of the through-wall cracks with crack length of 20% circumference the results obtained for the structural system case and for the component case also agreed very well. For all members the deviation of the results obtained for the structural system case is less than 1% when compared with the results calculated for the component case.

For through-wall cracks with a length of 40% circumference the results don't give a consistent indication. For the two members selected from the single braced jacket the results for the structural system case agree very well with the results obtained from the component case (less than 3%). In the case of the two members selected from the X-braced jacket the divergence of the results is somewhat larger (up to 8%) but the SIFs determined for the structural system case are smaller compared to the SIFs obtained for the component case. However, the discrepancy between the results of the two different approaches is still regarded as negligible.

For cracks with a length of 60% circumference and larger the SIFs calculated for the structural system case are significantly smaller than the SIFs calculated for the component case. The deviation is in the region of between 7% and 25% for cracks with a length of 60% circumference and approximately 50% for cracks with a length of 80% circumference. In this case, the reduction in section decreases the axial and bending stiffness of the member sufficiently such that stress redistribution in the structure occurs. The load attracted by the severed member therefore decreases.

It was shown that the beneficial effect of structural compliance on fatigue crack growth in the later stage of the growth process does not significantly increase the overall fatigue life. It was, therefore, concluded that the current approach, which uses stresses from undamaged structures to evaluate crack growth in individual components, is appropriate.

It has to be noted that these conclusions are based on a very limited set of results. Additionally, the assumption that the cracks develop in closure welds further limits the validity of the results. It is therefore recommended to increase the number of selected members and to extend the study to cracks in joint welds.

ACKNOWLEDGMENTS

The authors gratefully acknowledge the support provided by Dr. Alexander Stacey (Health & Safety Executive, UK). The authors also acknowledge the contribution of Mr John Sharples (Serco Assurance, UK) for providing technical advice to this study.

NOMENCLATURE

A	Constant in fatigue crack growth law (Paris law)
CHS	Circular hollow section
D	Outer diameter of circular hollow section
E	Young's modulus
FE	Finite Element (Method)
J	J-integral
LEFM	Linear Elastic Fracture Mechanics
K_1	Mode I Stress Intensity Factor for the component case (ignoring structural compliance)
K_2	Mode I Stress Intensity Factor for structural system case (including structural compliance)
ΔK_1	Mode I Stress Intensity Factor range for the component case (ignoring structural compliance)

ΔK_2	Mode I Stress Intensity Factor range for the structural system case (including structural compliance)
ΔP_m	Primary membrane stress range
R	Mean radius of circular hollow section
RLS	Reference Load Set
SIF or K_I	Mode I Stress Intensity Factor
a	Crack depth of semi-elliptical surface crack or half the crack length of through-wall crack
c	Half the crack length of semi-elliptical surface crack
l	Length of cracked component model
m	Exponent in fatigue crack growth law (Paris law)
r	Distance from crack tip
t	Wall thickness of circular hollow section
v	Poisson's ratio
da/dN	Crack growth rate with cycles

REFERENCES

[1] Nelson, A., Sanderson, D.J., and Stacey, A., 2002, "The Effects of Stress Redistribution due to Member Failure on Structural Reliability of Offshore Steel Jackets," OMAE2002-28612, *Proc. 21st International Conference on Offshore Mechanics and Artic Engineering*, Oslo, Norway

[2] BS 7910:2005, "Guide to methods for assessing the acceptability of flaws in metallic structures," British Standards Institution (BSI), UK

[3] ABAQUS/Standard v6.5, 2004, ABAQUS, Inc. USA

[4] ABAQUS/Aqua v5.8, 1998, ABAQUS, Inc. USA

[5] Sanderson, D.J., Price, A.G., Nelson, A., Thurlbeck, S.D., Killbourn, S., Dougan, A., 2002, "The Applicability of Online Monitoring for the Assurance of Fixed Jacket Structures' Structural Integrity," OMAE2002-28614, *Proc. 21st International Conference on Offshore Mechanics and Artic Engineering*, Oslo, Norway

[6] Schneider, R., and Sanderson, D.J., 2005, "Investigation of the Influence of Structural Compliance on Fatigue Life Predictions in Jacket Structures," Technical Report No. MMU041-R-01 Issue 1, MMI Engineering Ltd., Warrington, UK

[7] ABAQUS Analysis User's Manual, 2004, Verson 6.5, ABAQUS, Inc. USA

[8] Ewalds, H.L. and Wanhill R.J.H., 1989, "Fracture Mechanics," Edward Arnold, UK

[9] Al Laham, S., 1998, "Stress Intensity Factor and Limit Load Handbook," British Energy Generation Ltd., UK